\



Superconductivity in octagraphene

Jun Li(李军) and Dao-Xin Yao(姚道新)

Citation: Chin. Phys. B, 2022, 31 (**1**): 017403. DOI: 10.1088/1674-1056/ac40fa
Journal homepage: http://cpb.iphy.ac.cn; http://iopscience.iop.org/cpb

What follows is a list of articles you may be interested in

Majorana zero modes, unconventional real-complex transition, and mobility edges in a one-dimensional non-Hermitian quasi-periodic lattice

Shujie Cheng(成书杰) and Xianlong Gao(高先龙)
Chin. Phys. B, 2022, 31 (**1**): 017401. DOI: 10.1088/1674-1056/ac3222

Josephson current in an irradiated Weyl semimetal junction

Han Wang(王含) and Rui Shen(沈瑞)
Chin. Phys. B, 2021, 30 (**7**): 077406. DOI: 10.1088/1674-1056/ac0348

Temperature and doping dependent flat-band superconductivity on the Lieb-lattice

Feng Xu(徐峰), Lei Zhang(张磊), and Li-Yun Jiang(姜立运)
Chin. Phys. B, 2021, 30 (**6**): 067401. DOI: 10.1088/1674-1056/abdea5

Comparison of band structure and superconductivity in $FeSe_{0.5}Te_{0.5}$ and FeS

Yang Yang(杨阳), Shi-Quan Feng(冯世全), Yuan-Yuan Xiang(向圆圆), Hong-Yan Lu(路洪艳), Wan-Sheng Wang(王万胜)
Chin. Phys. B, 2017, 26 (**12**): 127401. DOI: 10.1088/1674-1056/26/12/127401

Electronic phase diagram of $NaFe_{1-x}Co_xAs$ investigated by scanning tunneling microscopy

Zhou Xiao-Dong, Cai Peng, Wang Ya-Yu
Chin. Phys. B, 2013, 22 (**8**): 087413. DOI: 10.1088/1674-1056/22/8/087413

TOPICAL REVIEW — Unconventional superconductivity

Superconductivity in octagraphene

Jun Li(李军)[1,2] and Dao-Xin Yao(姚道新)[1,†]

[1] *State Key Laboratory of Optoelectronic Materials and Technologies, School of Physics, Sun Yat-Sen University, Guangzhou* 510275, *China*
[2] *Key Laboratory for Microstructural Material Physics of Hebei Province, School of Science, Yanshan University, Qinhuangdao* 066004, *China*

(Received 17 September 2021; revised manuscript received 2 December 2021; accepted manuscript online 8 December 2021)

This article reviews the basic theoretical aspects of octagraphene, an one-atom-thick allotrope of carbon, with unusual two-dimensional (2D) Fermi nesting, hoping to contribute to the new family of quantum materials. Octagraphene has an almost strongest sp^2 hybrid bond similar to graphene, and has the similar electronic band structure as iron-based superconductors, which makes it possible to realize high-temperature superconductivity. We have compared various possible mechanisms of superconductivity, including the unconventional $s^{\pm}$ superconductivity driven by spin fluctuation and conventional superconductivity based on electron–phonon coupling. Theoretical studies have shown that octagraphene has relatively high structural stability. Although many 2D carbon materials with C_4 carbon ring and C_8 carbon ring structures have been reported, it is still challenging to realize the octagraphene with pure square-octagon structure experimentally. This material holds hope to realize new 2D high-temperature superconductivity.

Keywords: octagraphene, $s^{\pm}$ superconductivity, square-octagon lattice, Fermi surface nesting

PACS: 74.20.−z, 74.20.Pq, 74.70.Kn, 02.60.−x **DOI:** 10.1088/1674-1056/ac40fa

1. Introduction

As the chemical basis of the earth's biology, carbon widely exists in most substances of life. Fullerenes, carbon nanotubes, graphene, every breakthrough on carbon has been widely concerned by the scientific community. So, could they surprise superconductivity research? Graphene, as the first two-dimensional (2D) material, has attracted much attention in the field of superconductivity.[1–5] However, the hexagonal structure and electronic band properties of graphene make it difficult to produce superconductivity, or introduce low superconducting transition temperature (T_c).[5,6] In 2018, Cao *et al.* discovered superconductivity in magic-angle twisted bilayer-graphene.[7–10] However, due to the greatly reduced Fermi energy ($\sim$ 10 meV), its extremely low T_c limits its practical application. In addition to graphene, there are other isomers of carbon.[11] For example, although various forms of graphyne have been realized in experiments[12] which have the same hexagon symmetry with graphene, the superconductivity of graphyne has hardly come true.[13,14]

Recently, researchers found that octagraphene, a single-atom-thick allotrope of carbon composed of equal numbers of squares C_4 and octagons C_8, may have the natural p-orbital high-temperature superconductivity.[15,16] Fermi surfaces of octagraphene have hole pockets and electron pockets in the case of half-filled electrons to form perfect nesting, which is conducive to the formation of high-temperature p-orbital superconductivity based on spin fluctuation.[15] The theoretical calculations show that the superconducting energy gap of octagraphene ($\sim$ 50 meV) is similar to that of d-orbital cuprate superconductors.[17] Moreover, the Fermi velocity of octagraphene ($\sim 10^6$ m/s)[18] is much higher than that of d-orbital iron-based superconductors.[19,20] Therefore, the coherence length in octagraphene should be much longer than that in cuprate and iron-based superconductors, which is conducive to the realization of superconducting quantum computation.[21]

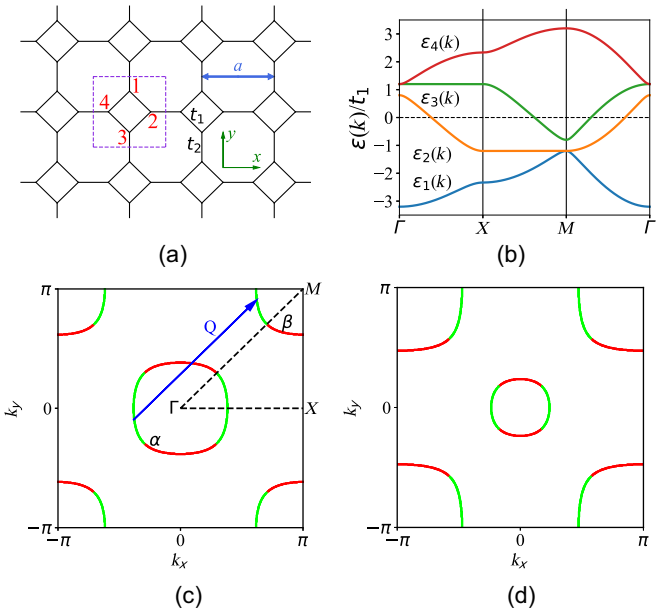


Fig. 1. (a) Sketch of the square-octagon lattice and illustration of the intrasquare nearest-neighbor hopping t_1 and the intersquare nearest-neighbor hopping t_2. The dotted square denotes the unit cell. (b) Band structure of the TB model (Eq. (1)) along the high symmetry lines in the first Brillouin zone. Panels (c) and (d) show the FSs of the undoped and 10% electron-doped cases, respectively. The site contributions on the FS sheets are shown by color: the red (green) represents that the weights contributed by the sublattices 1 and 3 (2 and 4) are dominant. The TB parameters are $t_1 = 1$, $t_2 = 1.2$. Adapted from Kang *et al.*[15]

†Corresponding author. E-mail: yaodaox@mail.sysu.edu.cn

© 2022 Chinese Physical Society and IOP Publishing Ltd

For the synthesis of 2D octagraphene group materials, different routes have been designed in theory,[22,23] and one-dimensional carbon nanoribbons with squares C_4 and octagons C_8 rings have been synthesized experimentally.[24] On this basis, the actual preparation of octagraphene can be expected.

In this paper, we present an overview and prospect on octagraphene. Emphasis will be given to the related correlated electron theory and numerical simulations carried out by our group during the past years. The outline of the paper is as follows. In Section 2, several different studies on carbon octagons and squares rings of octagraphene by means of the first-principles calculations are presented. The C_{4v} symmetry with versatile structurally favorable periodic sp^2 bonds is optimized using density functional perturbation theory (DFT). Section 3 is devoted to the theoretical model of the octagraphenes, including tight binding (TB) approximation and Hubbard model. Using the random-phase approximation (RPA), variation Monte Carlo (VMC) calculation and slave-boson mean field (SBMF) in Section 4, all three approaches consistently identify the single $s^{\pm}$-wave pairing as the leading pairing symmetry. Fabricating suggestions are given in some possible routes to synthesize octagraphene, and some recent progresses have been reported for the related 2D materials in a controllable manner in Section 5.

2. First-principles calculations

Octagraphene has been studied by several research groups and thus has different names. In 1994, Zhu *et al.* called octagraphene as imaginary "4:8 carbon plane net"[25] during the study of the conjugated-circuit computations on 2D carbon networks. Then in 2011, the family of 12 alternative 2D flat carbon networks was studied by Enyashin *et al.*, and octagraphene was examined as "network 7".[11] In 2012, Liu *et al.* found that octagraphene has Dirac-like fermions and a high Fermi velocity similar to graphene based on the first-principles calculations, and they called it "planer T-graphene".[18] Almost at the same time, inspired by the observations of line defects with octagons and pentagons, Sheng *et al.* proposed a stable 2D periodic atomic sheet consisting of carbon octagons, coined it as "octagraphene".[22] While studying a 84 set of Archimedean lattices in 2019, Crasto de Lima *et al.* reviewed the topological phases of octagraphene, named it "(4, 8_2) structure", and observed a $Z_2 = 0$ phase.[26] We here choose the name "octagraphene" with considering the octagons C_8 rings feature.

2.1. Geometrical structures

In general, as the first step, full geometry optimization was carried out for octagraphene. The lattice constant of the square cell is around $a_0 = 3.47$ Å, 3.45 Å, 3.42 Å, 3.446 Å and 3.444 Å, depending on different DFT methods.[11,16,22,23,26] Similar to graphene, every carbon atom in octagraphene has three sp^2-bonded nearest neighbors, forming three σ-bonds. In addition, octagraphene has two types of bond lengths, 1.48 Å (intra-squares) and 1.35 Å (inter-squares), and the bonds of each carbon atom have angles of one 90° and two 135°.[22] The relative positions of carbon atoms in a cell are almost independent of the lattice constant.[16] As shown in Fig. 2(b), the positions of four carbon atoms in a cell are (0.50a, 0.20a), (0.20a, 0.50a), (0.50a, 0.80a) and (0.80a, 0.50a) respectively, and consistent with C_{4v} symmetry, 2D space group $p4m$ or #11 ($p4mm$).

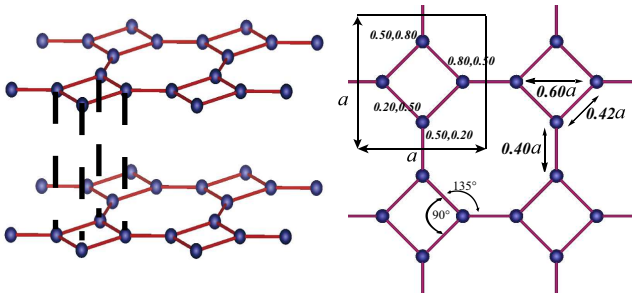


Fig. 2. Left: the predicted structure of octagraphene from DFT calculation. The relative positions between the layers form the A-A stacking. Right: structure of single-layer octagraphene. The relative positions of four carbon atoms in a unit cell are independent of the deformation. Adapted from Li *et al.*[16]

Besides, the situations of multi-layer octagraphene and bulk octagraphene (octagraphite) have also been studied.[16] Due to the C_{4v} symmetry of single-layer, there are three possibilities for stacking two octagraphene layers: A-A stacking, A-B stacking and A-C stacking. We find that the A-A stacking is the most stable compared to the other two. Otherwise from A-A stacking to A-B and A-C stacking, the energy gap is rarely small comparing with that for graphene. This indicates a weaker inter-layer coupling, making the material more slippery than graphite.[27] In other words, this reflects the 2D nature of octagraphite.

2.2. Band structures

The band structure shows that undoped octagraphene is metallic,[11,18] as shown in Fig. 3. More electrons are distributed on the inter-square bonds C_4 than on the intra-square bonds C_8 in octagraphene, showing an unequal sp^2 hybridization character. The top of valence band and the bottom of conduction band are located at the Γ and M points in the Brillouin zone, respectively. There is an indirect negative band gap about 4.03 eV,[22] leading to the Fermi level passing through both the conduction and valence bands. The band structures contain a hole pocket around the Γ point and an electron pocket around the M point, which is similar to those of cuprates,[17] iron-based superconductors,[20] and new found Ni-based superconductors.[28] The Γ and M points have C_{4v} symmetry, and the X point has C_{2v} symmetry, resulting in the doubly degenerate band structure on the Γ and M points. In

the ideal case, the two pockets connected by the perfect nesting vector $\boldsymbol{Q} = (\pi, \pi)$ form the perfect Fermi-surface nesting. On the other words, the hole and electron pockets share the same area.[16]

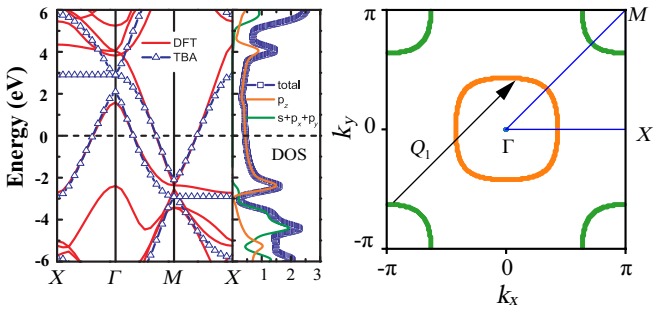


Fig. 3. Left: Electronic band structures and density of states (DOS) of octagraphene calculated by DFT and TB approximation. Adapted from Sheng *et al.*[22] Right: Fermi surface of octagraphene, where the hole packet (yellow) is at the Γ point, and the electron pocket (green) is at the M point. The Fermi surface is well nested by the vector $\boldsymbol{Q}_1 = (\pi, \pi)$.

The projected DOS of octagraphene shows that the energy bands near the Fermi surface are predominantly contributed by the $2p_z$ orbital of carbon atom. It is mostly dominated by the π bands, which is the same as that in graphene.[18,23] By neglecting the second and higher order terms, the Fermi velocity of octagraphene is estimated to be about $\sim 10^6$ m/s according to $v_F \simeq E(q)/|q|$,[23] which is close to the theoretical value of graphene[29] and higher than that of d-orbital iron-based superconductors.[19,20]

In Fig. 4, for larger lattice constant a, the electron orbits are more localized and have less overlap. The smaller lattice constant a leads to precipitous band structures and makes energy bands overlap with others. The nearly perfect Fermi-surface nesting is independent of the stress or strain along the layer.[16] The ultimate strain of octagraphene is about $1.3a_0$ to $1.4a_0$.[22] For $a/a_0 = 0.9$ in Fig. 4(c), the bands are quadruplely degenerate at the M point with $E = -3.01$ eV.[16] This coincidence is different from the Dirac point. The structure is not a bi-conical structure with linear dispersion, but a parabolic dispersion. It means that the low-energy excitations are no-longer massless.

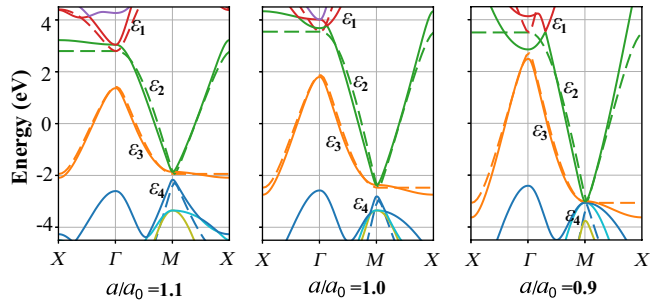


Fig. 4. Band structures of different lattice constant a: $a/a_0 = 1.1$, 1.0 and 0.9 [$a_0 = 3.44$ Å]. DFT calculated results, solid lines; fitting results obtained by TB model, dashed lines. For $a/a_0 = 0.9$, the bands show a quadruple degeneracy at the M point with $E = -3.01$ eV. From Li *et al.*[16]

For multi-layer octagraphene, each band of single-layer splits into multi bands due to the multiplied unit cell. As a result, there are several nesting hole pockets around the Γ point and several nesting electron pockets around the M point. For octagraphite, as shown in Fig. 5(a), the DFT calculated structure within a layer is almost the same as that of single-layer octagraphene, only slightly larger in size. There are always four bands near the Fermi level for a given k_z, which shows the 2D feature of octagraphene materials. The highest and the lowest boundaries of each band are marked by $k_z = 0$ and $k_z = \pi$, respectively. The 3D Fermi surface has a fusiform, where the largest hole pocket is around the Γ point. It also has similar spindle shape as those in cuprates,[17,30] iron-based superconductors,[20,31] and new found Ni-based superconductor family.[28]

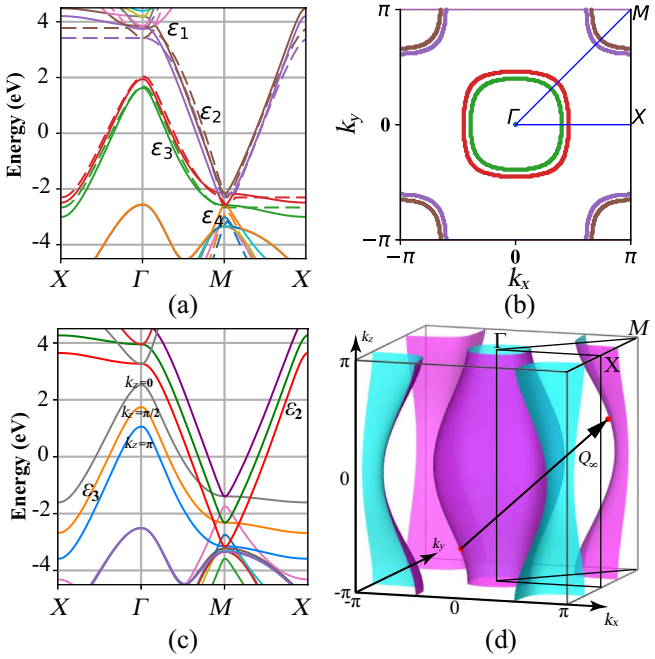


Fig. 5. (a) Band structures of the bi-layer octagraphene with $a_0 = 3.45$ Å. The solid lines represent the results by DFT calculation. The dashed lines are fitting results of TB model. (b) Fermi surface of bi-layer octagraphene. The nesting vectors $\boldsymbol{Q}_2 = (\pi, \pi)$, $(\pi + \delta, \pi + \delta)$ and $(\pi - \delta, \pi - \delta)$ mean the deviation of perfect Fermi surface nesting. (c) Band structures of octagraphite with $k_z = 0$, $\pi/2$, π. (d) Fermi surface of octagraphite, the nesting vector is almost $\boldsymbol{Q}_\infty = (\pi, \pi, \pi)$. Adapted from Li *et al.*[16]

2.3. Mechanical stability

According to the previous works,[18,22,23,26,32] no imaginary phonon modes are found in phonon spectra of octagraphene, implying that octagraphene is kinetically stable. The calculated total energy per atom of the octagraphene is 0.53, 0.52, 0.513, 0.50, 0.707 eV above graphene, depends on the different methods,[11,18,22,26,33] which is lower than the T-carbon ($\sim$ 1.31 eV),[34,35] graphdiyne ($\sim$ 0.77 eV),[36,37] graphyne ($\sim$ 0.66 eV)[38,39] and graphane ($\sim$ 2.99 eV),[40,41] all of which have already been experimentally obtained, suggesting that octagraphene is metastable against graphene. Molec-

ular dynamics simulations also indicate that octagraphene can hold stability even at a high temperature.[18,22,42–44]

The mechanical properties of octagraphene are also similar to those of graphene according to previous reports.[22,33,45,46] As it has a C_{4v} symmetry, two independent elastic constants are 296 N/m and 46 N/m, respectively. The Young's modulus E of octagraphene is obtained to be 306 N/m and 168 N/m along the two directions, respectively, in comparison to those of graphene (350 N/m).[47] The ultimate tensile strength or the breaking strength of octagraphene is 34.4 N/m and 27.3 N/m along the two directions, respectively, which are quite comparable with those of graphene (38.4 N/m, zigzag direction and 34.8 N/m, armchair direction).[47] The Poisson's ratios of octagraphene are 0.13 and 0.47 along the two directions, which are comparable with 0.21 (zigzag direction) and 0.17 (armchair direction) of graphene.[48] Octagraphene has the mechanical properties very similar to graphene and might be the strongest carbon atomic sheet after graphene till now.

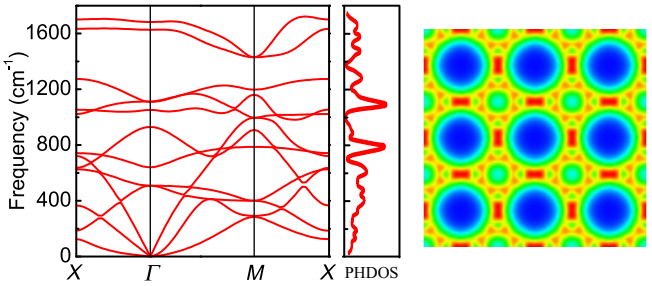


Fig. 6. Phonon dispersion and orbital projected band structure of octagraphene. Adapted from Lima *et al.*[26]

3. Models

3.1. TB model

As octagraphene has two types of bond lengths, the TB Hamiltonian for electrons in octagraphene has the form [16]

$$H_{\mathrm{TB}} = -\sum_{i,j,\sigma} t_{ij} c^{\dagger}_{i\sigma} c_{j\sigma} - \sum_{\langle i,j\rangle} t_{\perp} c^{\dagger}_{i} c_{j} + \mathrm{H.c.}, \tag{1}$$

where $c^{\dagger}_{i\sigma}$ ($c_{i\sigma}$) is the electron creation (annihilation) operator for a given site i with spin σ. t_{ij} (t_1, t_2 and t_3) correspond to hopping amplitudes of electrons between inter-square C_4 nearest-neighbor, intra-square C_8 nearest-neighbor and diagonal C_4 next nearest neighboring atoms, respectively. The $t_{\perp}$ represents the Van der Waals interlayer interaction between the neighbor layers. After a general procedure of Fourier transformation, the Hamiltonian of single-layer octagraphene reads as[16,22,49]

$$\widetilde{H}_1 = -\begin{bmatrix} 0 & t_1 & t_2 e^{ik_y} + t_3 & t_1 \\ t_1 & 0 & t_1 & t_2 e^{ik_x} + t_3 \\ t_2 e^{-ik_y} + t_3 & t_1 & 0 & t_1 \\ t_1 & t_2 e^{-ik_x} + t_3 & t_1 & 0 \end{bmatrix}. \tag{2}$$

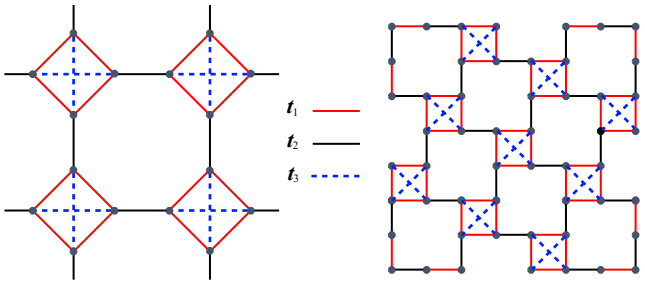


Fig. 7. The 2D single-orbital TB model. Left: square-octagon lattice. Right: 1/5 depleted square lattice. They are topologically equal. The t_1, t_2 and t_3 correspond to the intra-square, inter-square and diagonal hopping energies, respectively.

There are four bands ϵ_1, ϵ_2, ϵ_3 and ϵ_4 by diagonalizing the matrix Eq. (2). Based on the fittings,[16] the parameters should be $t_1 = 2.678 \pm 0.033$ eV, $t_2 = 2.9801 \pm 0.027$ eV and $t_3 = 0.548 \pm 0.024$ eV when $a/a_0 = 1.0$. Also some other fittings give $t_1 = 2.5$ eV and $t_2 = 2.9$ eV.[22] In comparison, $t \approx 2.7$ eV of the nearest-neighbor hopping energy and $t' \approx 0.1$ eV of the next nearest-neighbor hopping energy were reported in graphene.[29,50–52]

The t_3 is much smaller than t_1 and t_2 because the distance between the atoms along diagonal directions on squares is much longer than that of the nearest neighbors. As a result, t_3 is missing in the earlier studies.[15,22,26] Note that this small t_3 is necessary to split the ϵ_3 and ϵ_4 at the M point, and thus makes ϵ_2 to coincide with ϵ_3 here. In other words, if $t_3 = 0$, ϵ_3 and ϵ_4 overlap at the M point.

The values of t_1, t_2 decrease with the increase of a, but t_2/t_1 almost remains 1.1 when the a changes from $0.90a_0$ to $1.20a_0$. The p_z orbitals have an azimuthal symmetry, and therefore their interaction with neighbor p_z will be only distance dependent,[26] thus t_1/t_2 is independent of a and the Fermi surface stays unchanged. On the other hand, the TB model Eq. (1) is credible because of the well fits of the DFT calculated bands.[16]

For bulk octagraphite, the matrix form of the 3D TB model is written as

$$\widetilde{H}_{\infty} = -\begin{bmatrix} 2t_{\perp}\cos k_z & t_1 & t_2 e^{ik_y} + t_3 & t_1 \\ t_1 & 2t_{\perp}\cos k_z & t_1 & t_2 e^{ik_x} + t_3 \\ t_2 e^{ik_y} + t_3 & t_1 & 2t_{\perp}\cos k_z & t_1 \\ t_1 & t_2 e^{-ik_x} + t_3 & t_1 & 2t_{\perp}\cos k_z \end{bmatrix}, \tag{3}$$

in which $t_1 = 2.686 \pm 0.017$ eV, $t_2 = 2.986 \pm 0.013$ eV, $t_3 = 0.574 \pm 0.012$ eV and $t_{\perp} = 0.259 \pm 0.005$ eV from Li *et al.*'s fitting.[16] All t here have little difference from those in single-layer octagraphene. Notice that $t_{\perp}$ here is much smaller than that of graphene ($t_{\perp} \approx 0.4$ eV).[51]

Interestingly, in addition to the four energy bands near the Fermi level, other bands are almost the same and independent of the number of layers from the DFT results. These energy bands have almost no contribution to the interaction between layers, they are reflected by the local properties of orbit and have little influence for superconductivity.

Table 1. The lattice constant a_0, fitting parameters t_1, t_2, t_3, $t_\perp$ and λ of one to six layers of octagraphene and bulk octagraphite (∞).

	a_0 (Å)	t_1 (eV)	t_2 (eV)	t_3 (eV)	$t_\perp$ (eV)
1	3.444	2.678(33)	2.980(27)	0.548(24)	
2	3.446	2.685(21)	3.001(16)	0.558(16)	0.184(11)
3	3.447	2.680(16)	2.994(13)	0.548(12)	0.222(07)
4	3.446	2.678(13)	3.001(11)	0.550(11)	0.263(06)
5	3.447	2.671(12)	2.993(10)	0.546(09)	0.261(05)
6	3.449	2.677(11)	2.999(09)	0.548(08)	0.247(05)
∞	3.447	2.686(17)	2.986(13)	0.574(12)	0.259(05)

3.2. Hubbard model

Similar to graphene, there are Coulomb interactions between the $2p_z$ electrons in the octagraphene materials.[51,53,54] This local part of Coulomb interaction is also crucial for the theory of defect-induced magnetism in graphene.[55,56] The effective Hubbard model is used to describe the effects

$$H_{\text{Hubbard}} = H_{\text{TB}} + U\sum_i \hat{n}_{i\uparrow}\hat{n}_{i\downarrow}. \tag{4}$$

Here the U-term represents the effective on-site Coulomb interaction between the $2p_z$ electrons. There were some references in evaluating U in carbon-based materials, such as 16.9 eV in benzene,[53] 10 eV in polyacetylene[57,58] and 9.8 eV in graphene.[59]

This kind of octagraphene-like square-octagon lattice has been studied from different perspectives. The quantum phase transitions in square-octagon lattice were investigated by Kargarian *et al.*,[60] Bao *et al.*,[49,61] Sil *et al.*,[62] Lim *et al.*[26] and Pomata *et al.*[63] There are also applications in mathematical and theoretical computer science, such as packed loop models[64] and Markov chain.[65]

The square-octagon lattice was found in some other materials, such as octagon-structure monolayer of nitrogen,[66–68] $(10\bar{1}0)$ surfaces of ZnO,[69] alkaline iron selenide $A_2Fe_4Se_5$ $(A = \text{K, Rb, Cs, Tl})$,[70] magnetic CaV_4O_9 compound,[71] 2D transition metal dichalcogenides[72] and single-layer GaN and AlN.[73]

4. Superconductivity

For Hubbard model shown in Eq. (4), three different approaches used to treat the model with different limits of U give almost the same pairing symmetry and antiferromagnetic order. For the weak-, strong-, and intermediate-coupling strengths, the suitable calculations consistently yield standard $s^{\pm}$-wave superconductivity in this simple one-orbital system.

4.1. Weak-coupling limit

The standard multi-orbital RPA[74–86] approach was used to treat the weak-coupling limit of the model. The largest pairing eigenvalue λ is used to estimate T_c by the following equation:[79,87]

$$\lambda^{-1} = \ln\left(1.13\frac{\hbar\omega_{\text{D}}}{k_{\text{B}}T_{\text{c}}}\right), \tag{5}$$

here we choose the typical energy scale of spin fluctuation $\hbar\omega_{\text{D}} = 0.3$ eV in our calculation, see Ref. [87]. For the single-layer octagraphene, the largest eigenvalue of susceptibilities $\chi(\boldsymbol{q})$[79,84,85] over the Brillouin zone for the undoped case sharply peaks at $\boldsymbol{Q} = (\pi, \pi)$, reflecting the perfect Fermi surface nesting at that wave vector. The corresponding eigenvector $\xi(\boldsymbol{Q}) = (\frac{1}{2}, -\frac{1}{2}, \frac{1}{2}, -\frac{1}{2})$ reflects the intra-unit-cell fluctuation pattern, suggesting a Néel pattern.[15,88] With doping, the peak in the distribution of $\chi(\boldsymbol{q})$ deviates from $\boldsymbol{Q} = (\pi, \pi)$. The long range spin-density-wave order is destroyed when the doping concentration x further increases so that $U < U_{\text{c}}$.[84] Based on the antiferromagnetic spin fluctuations, the system is expected to realize standard $s^{\pm}$-pairing superconducting order.[15,85]

Eventually, $\lambda = 0.321$ for $a/a_0 = 1$ and $T_{\text{c}} \sim 190$ K are obtained for the single-layer octagraphene.[15,16] With decrease of a, T_{c} decreases in a limited scale. However, T_{c} would remain at very high level (> 100 K) whatever a is. In other words, single-layer octagraphene would be a good superconductor with limited mechanical deformation based on RPA.[16]

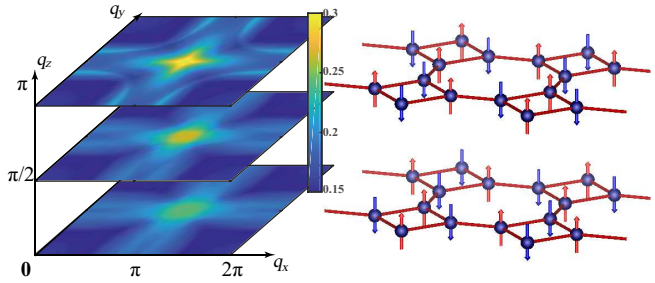


Fig. 8. Superconducting properties of octagraphite. Left: the eigen-susceptibilities $\chi(\boldsymbol{q})$ with $q_z = 0$, $\pi/2$, π. $\chi(\boldsymbol{q})$ peaks at almost $\boldsymbol{Q}_\infty = (\pi, \pi, \pi)$. Right: Predicted antiferromagnetic Néel pattern with half-filling. Adapted from Li *et al.*[16]

The $T_{\text{c}} \sim 170$ K is obtained for three to five layers and satuates at about 160 K for six layers and more, suggesting that superconductivity is mainly determined by the 2D characteristics of the material.[16] This phenomenon is similar to 2D high-temperature superconductivity, such as monolayer $Bi_2Sr_2CaCu_2O_{8+\delta}$.[89,90]

4.2. Intermediate-coupling

The RPA approach shows that superconductivity in octagraphene is unconventional and mediated by the antiferromagnetic spin fluctuations. However, as the effective superexchange parameter J for real materials with intermediate U is hard to study, T_{c} obtained here might not be accurate. In the following, the VMC approach was considered to study the problem[15,91]

$$|G\rangle = g^{\sum_i n_{i\uparrow}n_{i\ell}}\left(\sum_{k\alpha}\frac{v_k^\alpha}{u_k^\alpha}c_{k\alpha\uparrow}^\dagger c_{-k\alpha\downarrow}^\dagger\right)^{\frac{\Delta_{\text{s}}}{2}}|0\rangle. \tag{6}$$

Here $g \in (0,1)$ is the penalty factor of the double occupancy, N_e is the total number of electrons, and[92,93]

$$\frac{v_k^\alpha}{u_k^\alpha} = \frac{\Delta_k^\alpha}{\varepsilon_\alpha(k) + \sqrt{\varepsilon_\alpha^2(k) + |\Delta_k^\alpha|^2}}, \tag{7}$$

where $\Delta_k^\alpha = \Delta^\alpha f(k)$ is the superconducting gap function. Here only intra-band pairings on the $\alpha = 2$, 3 bands crossing the Fermi surface are considered.

The δ dependence of the energy per unit cell for each form factor is shown in Fig. 5(a) for $U = 4t_1 = 10$ eV for a typical doping $x = 10\%$, with g and μ_c optimized for each δ. Note that the optimized $g = 0.5475$ is almost equal to the optimized value without SC, and that μ_c is almost equal to the value obtained in the mean-field calculation. From Fig. 9(a), one finds that the $s^{\pm}$-wave pairing causes the most energy gain among the four gap form factors, with the optimized gap amplitude at $\delta = 0.022t_1 \simeq 50$ meV, comparable with cuprates, implying similar T_c between them. The gap function of the $s^{\pm}$-wave SC obtained is shown on the Fermi surface in Fig. 9(b), which is well consistent with that obtained in the RPA calculation.[15]

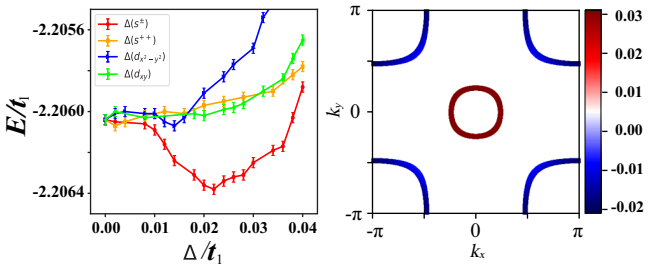


Fig. 9. The VMC results. Left: energy per unit cell as function of δ for the four different gaps. Right: the $s^{\pm}$-wave gap function projected on the Fermi surface. Adapted from Kang *et al.*[15]

4.3. Strong-coupling limit

In the strong-coupling limit, the Hubbard model becomes an effective t–J model[86]

$$H_{AF} = \sum_{\langle i,j \rangle} J_{i,j} \widehat{S}_i \cdot \widehat{S}_j, \tag{8}$$

where $\widehat{S}_i$ is the electron spin, and $J = 2t^2/U$.[94] This Hamiltonian should be understood as acting on the subspace of empty (double-occupancy) and single occupied sites for the hole-doped (electron-doped) system.

In the SBMF approach[94–101] with the effective t–J model, the electron operator $c_{i\sigma}$ can be replaced by $c_{i\sigma} \to f_{i\sigma} b_i^\dagger$, with the bosonic holon (doublon) operator $b_i^\dagger$ and the fermionic spinon operator $f_{i\sigma}$ subject to the no-double-occupancy constraint $b_i^\dagger b_i + \sum_\sigma f_{i\sigma}^\dagger f_{i\sigma} = 1$ enforced by the Lagrange multiplier.[94] At zero temperature the condensation of bosonic $b_i^\dagger$ leads to $b_i^\dagger \to \sqrt{x}$ and left with only the fermionic $f_{i\sigma}$ degree of freedom. The quartic term of $f_{i\sigma}$ is further mean-field decomposed with the following two mean-field order parameters:[95]

$$\begin{aligned} \kappa_{(i,j)} &= \left\langle f_{j\uparrow}^\dagger f_{i\uparrow} \right\rangle = \left\langle f_{j\downarrow}^\dagger f_{i\downarrow} \right\rangle, \\ \Delta_{(i,j)} &= \left\langle f_{j\downarrow} f_{i\uparrow} - f_{j\uparrow} f_{i\downarrow} \right\rangle. \end{aligned} \tag{9}$$

Two mean-field $\kappa_{(i,j)}(\Delta_{(i,j)})$ parameters are obtained by solving the mean-field equations self-consistently.[95] The $s^{\pm}$-wave SC gains more energy and becomes the ground state, verifies the standard $s^{\pm}$-pairing state, which is well consistent with the gap function obtained by RPA.[15]

The doping-dependence of the superconducting order deviation parameter $\Delta_{(i,j)}^{(c)} = \langle c_{j\downarrow} c_{i\uparrow} - c_{j\uparrow} c_{i\downarrow} \rangle = x\Delta_{(i,j)}$ is shown in Fig. 10(b), which illustrates a cuprates-like dome. By using BCS relation $2J\delta^{(c)}/T_c \simeq 3.53$, $T_c \simeq 180$ K was obtained near $x = 10\%$.[15]

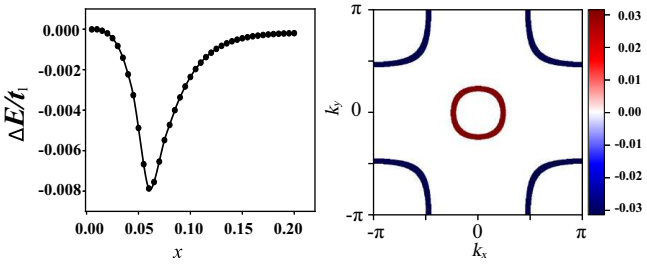


Fig. 10. The SBMF results. Left: doping dependence of the energy (per unit cell) difference between the $s^{\pm}$-wave pairing and the d-wave one, $\Delta E = E_s - E_d$, in units of t_1. Right: the $s^{\pm}$-wave gap function projected on the Fermi surface. Adapted from Kang *et al.*[15]

4.4. More discussion

The Heisenberg Hamiltonian Eq. (8) for square-octagon lattice (or 1/5-depleted square lattice) has been widely studied since the realization of CaV_4O_9.[71,102–107] Magnetic phase diagram and Mott transition were found with frustrations.[108–114] Then this magnetic structure was also realized in alkaline iron selenide $A_2Fe_4Se_5$ (A = K, Rb, Cs, Tl) single crystals.[70,115]

In 2019, Gu *et al.* investigated superconducting properties of octagraphene based on electron–phonon coupling and Allen–Dynes modified McMillian equation.[116] From BCS theory, they obtained T_c up to around 20.8 K at ambient pressure.[23,117] In 2020, Nunes *et al.* found flat-band superconductivity[118] for tight-binding electrons on square-octagon lattice. Similar to twisted bilayer graphene, they suggested that T_c might reach a high value.[119] Interestingly, when consider the similar 1/5-depleted square lattice Hubbard Model at half-filling, the dominant pairing symmetry changes character from d wave in the plaquette phase to an extended s wave in the Néel phase,[88] revealing a good agreement with octagraphene.

We notice that the bi-layer octagraphene can enter the superconducting state by applying a vertical electric field between the layers even without doping.[120] This will greatly facilitate the manipulation of superconductivity. All these stud-

ies have come to the same conclusion: octagraphene could be a good platform for high-T_c superconductivity.

5. Experimental realization

5.1. Synthetic progress

So far there are already some octagraphene related materials reported. Similar to carbon nanoribbons, octagraphene nanoribbons rolled from octagraphene were predicted to be mechanically stable and promising for the development of electromagnetic radiation sensors.[22,121–123] When the C_4 of the octagraphene layers are bonded to each other, the bulk T-graphene similar to octagraphite was predicted to have a high Fermi velocity.[18,124,125] The 2D Dirac material S-graphyne was found to contain two sizes of squares C_4 rings,[126] similar to both graphyne and octagraphene. Moreover, square-octagon pair (4|8) was also discovered in 2D boron nitride (h-BN).[127–129]

Finally, let us look back to the progress in octagraphene experimental synthesis. The separate square C_4 rings[130,131] and octagon C_8 rings[131] were realized long ago chemically. The C_8-C_5 sp^2-hybridized carbon rings were realized by one-dimensional topological defects in graphene.[132–134] The C_4-C_6 cyclic dehydrogenative C–C coupling was obtained using on-surface synthesis.[135,136] Graphene-like nanoribbons periodically embedded with C_4-C_8 structures were fabricated successfully on Au(111).[24]

In 2021, Fan *et al.* synthesized an ultraflat biphenylene carbon sheet consisting of sp^2-hybridized carbon atoms forming C_4, C_6 and C_8 on a gold surface.[137] The 2D biphenylene sheet presents a metallic character, and also in the planar strips with zigzag-type edges. Armchair-edged strips develop a band gap that decreases monotonically with the ribbon width.[138–140] We have found that this material has a C_4-C_8 structure in just one direction and the remaining C_6 structure may be harmful to the superconductivity.[120]

5.2. Fabricating routes

Octagraphene has similar mechanical properties as graphene[47] and might be the strongest carbon atomic sheet after graphene till now according to previous reports.[22,33,45] However, directly rotating C–C bonds from graphene lattice to octagraphene has a huge energy barrier (up to 7 eV).[141] Moreover, these processes from honeycomb and square-octagon lattices were examined to be quite hard by kinetic Monte Carlo simulations.[142]

There were four theoretical synthetic routes reported for octagraphene.[22,23,47,143] One route is to make the line defects periodically in graphene and then connect properly the broken bonds of carbon atoms.[22] The second route is to use large uniaxial stress beyond the fracture limit[47] to convert graphene to two periodic pentaheptite structures, then further into octagraphene. The third route suggests to exfoliate the bulk C_4K, C_4Li or C_4Na with similar electrochemical method used in graphite intercalation compounds.[1,23,144,145] The last one proposes an atom-mimicking design concept to achieve direct self-assembly of 2D low-coordinated open lattices to compose octagraphene.[143] Other synthetic routes to realize octagraphene are possible.

6. Conclusions

In summary, an overview on the progress of superconductivity in the octagraphene has been presented. The geometrical and band structures of octagraphene show more 2D characteristic than that of graphene and can hold mechanical stability even at high temperature. Octagraphene is believed to be an ideal system to study superconductivity. The perfect Fermi surface nesting from undoped octagraphene can induce the long-ranged SDW order. Upon doping or applying a vertical electrical field on the multi-layer octagraphene, high T_c superconductivity is expected. The RPA, VMC, and SBMF approaches for the weak-, intermediate-, and strong-coupling strengths consistently yield the standard $s^{\pm}$-wave superconductivity, respectively. Besides, octagraphene may have traditional p-orbital superconductivity with considerable T_c based on the electron–phonon coupling calculations. These mechanisms may coexist in octagraphene for realizing the possible high T_c superconductivity. So far, there were already experiments which can realize 2D carbon materials with square C_4 rings and octagon C_8 rings structures. For example, an ultraflat biphenylene carbon sheet consisting of C_4-C_6-C_8 was synthesized recently. Theoretically, at leat four synthetic routes were reported for octagraphene, and new surface synthesis route is on the way. Furthermore, octagraphene is supposed to have long superconducting coherence time based on its 2D nature and large Fermi velocity from p-orbitals, which is conducive to quantum computation.

Acknowledgments

This project is supported by the National Key R&D Program of China (Grant Nos. 2017YFA0206203 and 2018YFA0306001), the National Natural Science Foundation of China (Grant No. 11974432), GBABRF-2019A1515011337, Natural Science Foundation of Hebei Province, China (Grant No. A2021203010), Shenzhen Institute for Quantum Science and Engineering (Grant No. SIQSE202102), and Leading Talent Program of Guangdong Special Projects.

References

[1] Calandra M, Profeta G and Mauri F 2012 *Physica Status Solidi (b)* **249** 2544

[2] Pešić J, Gajić R, Hingerl K and Belić M 2014 *Europhys. Lett.* **108** 67005
[3] Kaloni T P, Balatsky A V and Schwingenschlögl U 2013 *Europhys. Lett.* **104** 47013
[4] Mazin I and Balatsky A 2010 *Philosophical Magazine Letters* **90** 731
[5] Si C, Liu Z, Duan W and Liu F 2013 *Phys. Rev. Lett.* **111** 196802
[6] Zhang D Bo, Han Q and Wang Z D 2013 *Chin. Phys. Lett.* **30** 057401
[7] Cao Y, Fatemi V, Fang S, Watanabe K, Taniguchi T, Kaxiras E and Jarillo-Herrero P 2018 *Nature* **556** 43
[8] Zhang M, Zhang Y, Lu C, Chen W Q and Yang F 2020 *Chin. Phy. B* **29** 127102
[9] Chu Y, Zhu F, Wen L, Chen W, Chen Q and Ma T 2020 *Chin. Phy. B* **29** 117401
[10] Liu Z, Li Y and Yang Y F 2019 *Chin. Phy. B* **28** 077103
[11] Enyashin A N and Ivanovskii A L 2011 *Physica Status Solidi (b)* **248** 1879
[12] Malko D, Neiss C, Viñes F and Görling A 2012 *Phys. Rev. Lett.* **108** 086804
[13] Morshedloo T, Roknabadi M R, Behdani M, Modarresi M and Kazempour A 2016 *Computational Materials Science* **124** 183
[14] Xu F and Zhang L 2019 *Chin. Phy. B* **28** 117403
[15] Kang Y T, Lu C, Yang F and Yao D X 2019 *Phys. Rev. B* **99** 184506
[16] Li J, Jin S, Yang F and Yao D X 2020 *Phys. Rev. B* **102** 174509
[17] Damascelli A, Hussain Z and Shen Z X 2003 *Rev. Mod. Phys.* **75** 473
[18] Liu Y, Wang G, Huang Q, Guo L and Chen X 2012 *Phys. Rev. Lett.* **108** 225505
[19] Stewart G R 2011 *Rev. Mod. Phys.* **83** 1589
[20] Yamashita M, Senshu Y, Shibauchi T, Kasahara S, Hashimoto K, Watanabe D, Ikeda H, Terashima T, Vekhter I, Vorontsov A B and Matsuda Y 2011 *Phys. Rev. B* **84** 060507
[21] Li J S, Li Z B and Yao D X 2012 *Chin. Phy. B* **21** 017302
[22] Sheng X L, Cui H J, Ye F, Yan Q B, Zheng Q R and Su G 2012 *J. Appl. Phys.* **112** 074315
[23] Qinyan Gu Dingyu Xing J S 2019 *Chin. Phys. Lett.* **36** 097401
[24] Liu M, Liu M, She L, Zha Z, Pan J, Li S, Li T, He Y, Cai Z, Wang J, Zheng Y, Qiu X and Zhong D 2017 *Nat. Commun.* **8** 14924
[25] Zhu H, Balaban A T, Klein D J and Zivkovic T P 1994 *J. Chem. Phys.* **101** 5281
[26] Lima F C d, Ferreira G J and Miwa R H 2019 *Phys. Chem. Chem. Phys.* **21** 22344
[27] Liu Z 2014 *Nanotechnology* **25** 075703
[28] Li D, Lee K, Wang B Y, Osada M, Crossley S, Lee H R, Cui Y, Hikita Y and Hwang H Y 2019 *Nature* **572** 624
[29] Deacon R S, Chuang K C, Nicholas R J, Novoselov K S and Geim A K 2007 *Phys. Rev. B* **76** 081406
[30] Tsuei C C and Kirtley J R 2000 *Rev. Mod. Phys.* **72** 969
[31] Jiang Q, Kang Y T and Yao D X 2013 *Chin. Phy. B* **22** 087402
[32] Li D, Jiang L, Zhu M and Zheng Y 2020 *Solid State Commun.* **322** 114064
[33] Andrew R C, Mapasha R E, Ukpong A M and Chetty N 2012 *Phys. Rev. B* **85** 125428
[34] Sheng X L, Yan Q B, Ye F, Zheng Q R and Su G 2011 *Phys. Rev. Lett.* **106** 155703
[35] Xu K, Liu H, Shi Y C, You J Y, Ma X Y, Cui H J, Yan Q B, Chen G C and Su G 2020 *Carbon* **157** 270
[36] Haley M M 2008 *Pure and Applied Chemistry* **80** 519
[37] Li G, Li Y, Liu H, Guo Y, Li Y and Zhu D 2010 *Chemical Communications* **46** 3256
[38] Malko D, Neiss C, Viñes F and Görling A 2012 *Phys. Rev. Lett.* **108** 086804
[39] Kehoe J M, Kiley J H, English J J, Johnson C A, Petersen R C and Haley M M 2000 *Organic Letters* **2** 969
[40] Elias D C, Nair R R, Mohiuddin T M G, Morozov S V, Blake P, Halsall M P, Ferrari A C, Boukhvalov D W, Katsnelson M I, Geim A K and Novoselov K S 2009 *Science* **323** 610
[41] Sofo J O, Chaudhari A S and Barber G D 2007 *Phys. Rev. B* **75** 153401
[42] Ye X J, Liu C S, Zhong W, Zeng Z and Du Y W 2014 *J. Appl. Phys.* **116** 114304
[43] He C and Wang W 2020 *Nanomaterials* **10** 2252
[44] Podlivaev A I and Openov L A 2013 *Physics of the Solid State* **55** 2592
[45] Fthenakis Z G and Lathiotakis N N 2015 *Phys. Chem. Chem. Phys.* **17** 16418
[46] Shang M, ling Li P, hua Wang Y and wei Luo J 2021 *Chin. Phy. B* **30** 80703
[47] Lee C, Wei X, Kysar J W and Hone J 2008 *Science* **321** 385
[48] Majidi R 2017 *Theoretical Chemistry Accounts* **136** 109
[49] Bao A, Tao H S, Liu H D, Zhang X and Liu W M 2014 *Scientific Reports* **4** 6918
[50] Reich S, Maultzsch J, Thomsen C and Ordejón P 2002 *Phys. Rev. B* **66** 035412
[51] Castro Neto A H, Guinea F, Peres N M R, Novoselov K S and Geim A K 2009 *Rev. Mod. Phys.* **81** 109
[52] Ijas M and Harju A 2010 *Phys. Rev. B* **82** 235111
[53] Parr R G, Craig D P and Ross I G 1950 *J. Chem. Phys.* **18** 1561
[54] Schüler M, Rösner M, Wehling T O, Lichtenstein A I and Katsnelson M I 2013 *Phys. Rev. Lett.* **111** 036601
[55] Shibayama Y, Sato H, Enoki T and Endo M 2000 *Phys. Rev. Lett.* **84** 1744
[56] López-Sancho M P, de Juan F and Vozmediano M A H 2009 *Phys. Rev. B* **79** 075413
[57] Vardeny Z and Tauc J 1985 *Phys. Rev. Lett.* **54** 1844
[58] Baeriswyl D, Campbell D K and Mazumdar S 1986 *Phys. Rev. Lett.* **56** 1509
[59] Wehling T O, Sasiolu E, Friedrich C, Lichtenstein A I, Katsnelson M I and Blügel S 2011 *Phys. Rev. Lett.* **106** 236805
[60] Kargarian M and Fiete G A 2010 *Phys. Rev. B* **82** 085106
[61] Bao A, Zhang X F and Zhang X Z 2015 *Chin. Phy. B* **24** 050310
[62] Sil A and Ghosh A K 2019 *J. Phys.: Condens. Matter* **31** 245601
[63] Pomata N and Wei T C 2020 *Phys. Rev. Lett.* **124** 177203
[64] Jacobsen J L 1999 *J. Phys. A: Math. Gen.* **32** 5445
[65] Bhakta P and Randall D 2017 *Theoretical Computer Science* **699** 21
[66] Zhang Y, Lee J, Wang W L and Yao D X 2015 *Computational Materials Science* **110** 109
[67] Lin W, Liang S D, He C, Xie W, He H, Mai Q, Li J and Yao D X 2019 *Scientific Reports* **9** 1025
[68] Ersan F, Kecik D, Ozcelik V O, Kadioglu Y, Akturk O U, Durgun E, Akturk E and Ciraci S 2019 *Appl. Phys. Rev.* **6** 021308
[69] He M R, Yu R and Zhu J 2012 *Angewandte Chemie* **124** 7864
[70] Ye F, Chi S, Bao W, Wang X F, Ying J J, Chen X H, Wang H D, Dong C H and Fang M 2011 *Phys. Rev. Lett.* **107** 137003
[71] Troyer M, Kontani H and Ueda K 1996 *Phys. Rev. Lett.* **76** 3822
[72] Li X, Zhang S and Wang Q 2017 *Nanoscale* **9** 562
[73] Gurbuz E, Cahangirov S, Durgun E and Ciraci S 2017 *Phys. Rev. B* **96** 205427
[74] Graser S, Kemper A F, Maier T A, Cheng H P, Hirschfeld P J and Scalapino D J 2010 *Phys. Rev. B* **81** 214503
[75] Kubo K 2007 *Phys. Rev. B* **75** 224509
[76] Luo Q, Martins G, Yao D X, Daghofer M, Yu R, Moreo A and Dagotto E 2010 *Phys. Rev. B* **82** 104508
[77] Ma T, Yang F, Yao H and Lin H Q 2014 *Phys. Rev. B* **90** 245114
[78] Wu X, Yang F, Le C, Fan H and Hu J 2015 *Phys. Rev. B* **92** 104511
[79] Zhang L D, Yang F and Yao Y 2015 *Scientific Reports* **5** 8203
[80] Kontani H and Ueda K 1998 *Phys. Rev. Lett.* **80** 5619
[81] Kuroki K, Kimura T, Arita R, Tanaka Y and Matsuda Y 2002 *Phys. Rev. B* **65** 100516
[82] Yamada K, Lee C H, Kurahashi K, Wada J, Wakimoto S, Ueki S, Kimura H, Endoh Y, Hosoya S, Shirane G, Birgeneau R J, Greven M, Kastner M A and Kim Y J 1998 *Phys. Rev. B* **57** 6165
[83] Maier T A, Graser S, Hirschfeld P J and Scalapino D J 2011 *Phys. Rev. B* **83** 100515
[84] Mazin I I, Singh D J, Johannes M D and Du M H 2008 *Phys. Rev. Lett.* **101** 057003
[85] Graser S, Maier T A, Hirschfeld P J and Scalapino D J 2009 *New J. Phys.* **11** 025016
[86] Wu H Q, He R Q, Meng Z Y and Lu Z Y 2015 *Phys. Rev. B* **91** 125128
[87] Liu F, Liu C C, Wu K, Yang F and Yao Y 2013 *Phys. Rev. Lett.* **111** 066804
[88] Khatami E, Singh R R, Pickett W E and Scalettar R T 2014 *Phys. Rev. Lett.* **113** 106402
[89] Chatterjee U, Shi M, Ai D, Zhao J, Kanigel A, Rosenkranz S, Raffy H, Li Z Z, Kadowaki K, Hinks D G, Xu Z J, Wen J S, Gu G, Lin C T, Claus H, Norman M R, Randeria M and Campuzano J C 2010 *Nat. Phys.* **6** 99

[90] Yu Y, Ma L, Cai P, Zhong R, Ye C, Shen J, Gu G D, Chen X H and Zhang Y 2019 *Nature* **575** 156
[91] Yang F, Zhai H, Wang F and Lee D H 2011 *Phys. Rev. B* **83** 134502
[92] Umrigar C J, Wilson K G and Wilkins J W 1988 *Phys. Rev. Lett.* **60** 1719
[93] Ceperley D, Chester G V and Kalos M H 1977 *Phys. Rev. B* **16** 3081
[94] Kotliar G and Liu J 1988 *Phys. Rev. B* **38** 5142
[95] Kopp T, Seco F J, Schiller S and Wolfle P 1988 *Phys. Rev. B* **38** 11835
[96] Meyer R and Entel P 1993 *Phys. Rev. B* **47** 1099
[97] Bul/ka B R and Robaszkiewicz S 1996 *Phys. Rev. B* **54** 13138
[98] Ribeiro T C and Wen X G 2008 *Phys. Rev. B* **77** 144526
[99] Bünemann J 2011 *Physica Status Solidi (b)* **248** 203
[100] Klett M, Ok S, Riegler D, Wölfle P, Thomale R and Neupert T 2020 *Phys. Rev. B* **101** 161112
[101] Riegler D, Klett M, Neupert T, Thomale R and Wolfle P 2020 *Phys. Rev. B* **101** 235137
[102] White S R 1996 *Phys. Rev. Lett.* **77** 3633
[103] Sachdev S and Read N 1996 *Phys. Rev. Lett.* **77** 4800
[104] Weihong Z, Gelfand M P, Singh R R P, Oitmaa J and Hamer C J 1997 *Phys. Rev. B* **55** 11377
[105] Bose I and Ghosh A 1997 *Phys. Rev. B* **56** 3149
[106] Manuel L O, Micheletti M I, Trumper A E and Ceccatto H A 1998 *Phys. Rev. B* **58** 8490
[107] Farnell D J J, Schulenburg J, Richter J and Gernoth K A 2005 *Phys. Rev. B* **72** 172408
[108] Ng K K 2010 *Phys. Rev. B* **81** 094426
[109] Yamashita Y, Tomura M, Yanagi Y and Ueda K 2013 *Phys. Rev. B* **88** 195104
[110] Yanagi Y and Ueda K 2014 *Phys. Rev. B* **90** 085113
[111] Yamada A 2014 *Phys. Rev. B* **90** 245139
[112] Iglovikov V I, Khatami E and Scalettar R T 2015 *Phys. Rev. B* **92** 045110
[113] Zhang L and Wang F 2017 *Phys. Rev. Lett.* **118** 087201
[114] Liu Y J, Chen Y C, Yang M F and Gong C D 2006 *J. Phys.: Condens. Matter* **18** 1805
[115] Bao W, Huang Q Z, Chen G F, Wang D M, He J B and Qiu Y M 2011 *Chin. Phys. Lett.* **28** 086104
[116] Allen P B and Dynes R C 1975 *Phys. Rev. B* **12** 905
[117] Ma Y M 2019 *Chin. Phys. Lett.* **36** 90101
[118] Pal B 2018 *Phys. Rev. B* **98** 245116
[119] Nunes L H C M and Smith C M 2020 *Phys. Rev. B* **101** 224514
[120] Ye J, Li J and Yao D X, In preparation
[121] Sergeyev D M, Myasnikova L N and Shunkeyev K S 2020 *Russian Physics Journal* **63** 303
[122] Kochaev A I, Meftakhutdinov R M, Sibatov R T and Timkaeva D A 2021 *Computational Materials Science* **186** 109999
[123] Li F, Lu J, Zhu H and Lin X 2018 *Results in Physics* **9** 656
[124] Huang H, Li Y, Liu Z, Wu J and Duan W 2013 *Phys. Rev. Lett.* **110** 029603
[125] Kim B G, Jo J Y and Sim H S 2013 *Phys. Rev. Lett.* **110** 029601
[126] Zhang L Z, Wang Z F, Wang Z M, Du S X, Gao H J and Liu F 2015 *The Journal of Physical Chemistry Letters* **6** 2959
[127] Liu Y, Zou X and Yakobson B I 2012 *ACS Nano* **6** 7053
[128] Cretu O, Lin Y C and Suenaga K 2014 *Nano Lett.* **14** 1064
[129] Li Q, Zou X, Liu M, Sun J, Gao Y, Qi Y, Zhou X, Yakobson B I, Zhang Y and Liu Z 2015 *Nano Lett.* **15** 5804
[130] Jiao H, Schleyer P v R, Mo Y, McAllister M A and Tidwell T T 1997 *J. Am. Chem. Soc.* **119** 7075
[131] Slayden S W and Liebman J F 2001 *Chemical Reviews* **101** 1541
[132] Lahiri J, Lin Y, Bozkurt P, Oleynik I I and Batzill M 2010 *Nat. Nanotech.* **5** 326
[133] Kotakoski J, Krasheninnikov A V, Kaiser U and Meyer J C C 2011 *Phys. Rev. Lett.* **106** 105505
[134] Cai XH, Yang Q, Zheng S and Wang M 2021 *Energy Environ. Mater.* **4** 458
[135] Fan Q, Martin-Jimenez D, Ebeling D, Krug C K, Brechmann L, Kohlmeyer C, Hilt G, Hieringer W, Schirmeisen A and Gottfried J M 2019 *J. Am. Chem. Soc.* **141** 17713
[136] Zhang R, Xia B, Xu H and Lin N 2019 *ChemPhysChem* **20** 2292
[137] Fan Q, Yan L, Tripp M W, Krejčí O, Dimosthenous S, Kachel S R, Chen M, Foster A S, Koert U, Liljeroth P and Gottfried J M 2021 *Science* **372** 852
[138] Hudspeth M A, Whitman B W, Barone V and Peralta J E 2010 *ACS Nano* **4** 4565
[139] Karaush N N, Baryshnikov G V and Minaev B F 2014 *Chem. Phys. Lett.* **612** 229
[140] Ma Y B, Ouyang T, Chen Y P and Xie Y E 2021 *Chin. Phy. B* **30** 77103
[141] Crespi V H, Benedict L X, Cohen M L and Louie S G 1996 *Phys. Rev. B* **53** R13303
[142] Zhang Z, Xun Z, Wu L, Chen Y, Xia H, Hao D and Tang G 2017 *Euro. Phys. J. B* **90** 89
[143] Li Z W, Sun Y W, Wang Y H, Zhu Y L, Lu Z Y and Sun Z Y 2020 *Nanoscale* **12** 4544
[144] Hu J, Liu Y, Liu N, Li J and Ouyang C 2020 *Phys. Chem. Chem. Phys.* **22** 3281
[145] Zhang X, Jin L, Dai X, Chen G and Liu G 2020 *Appl. Surf. Sci.* **527** 146849